1-11-2021

Competitive formation of intercalated versus supported metal nanoclusters during deposition on layered materials with surface point defects

Yong Han
Ames Laboratory, y27h@iastate.edu

Ann Lii-Rosales
Iowa State University and Ames Laboratory

Michael C. Tringides
Iowa State University and Ames Laboratory, mctringi@ameslab.gov

James W. Evans
Iowa State University, jevans@ameslab.gov

Competitive formation of intercalated versus supported metal nanoclusters during deposition on layered materials with surface point defects

Abstract

Intercalated metal nanoclusters (NCs) can be formed under the surface of graphite after sputtering to generate surface “portal” defects that allow deposited atoms to reach the subsurface gallery. However, there is a competition between formation of supported NCs on top of the surface and intercalated NCs under the surface, the latter only dominating at sufficiently high temperature. A stochastic model incorporating appropriate system thermodynamics and kinetics is developed to capture this complex and competitive nucleation and growth process. Kinetic Monte Carlo simulation shows that the model captures experimental trends observed for Cu and other metals and reveals that higher temperatures are needed to facilitate detachment of atoms from supported NCs enabling them to reach the gallery.

Disciplines

Biological and Chemical Physics | Nanoscience and Nanotechnology

Competitive formation of intercalated versus supported metal nanoclusters during deposition on layered materials with surface point defects

Yong Han,[1,2] Ann Lii-Rosales,[1,3,*] Michael C. Tringides,[1,2] and James W. Evans[1,2]

[1]Ames Laboratory, U. S. Department of Energy, Ames, Iowa 50011, USA
[2]Department of Physics and Astronomy, Iowa State University, Ames, Iowa 50011, USA
[3]Department of Chemistry, Iowa State University, Ames, Iowa 50011, USA

*Current address: Department of Chemistry, University of Colorado Boulder, Boulder, CO 80309

ABSTRACT

Intercalated metal nanoclusters (NCs) can be formed under the surface of graphite after sputtering to generate surface "portal" defects which allow deposited atoms to reach the subsurface gallery. However, there is a competition between formation of supported NCs on top of the surface and intercalated NCs under the surface, the latter only dominating at sufficiently high temperature. A stochastic model incorporating appropriate system thermodynamics and kinetics is developed to capture this complex and competitive nucleation and growth process. KMC simulation shows that the model captures experimental trends observed for Cu and other metals, and reveals that higher temperatures are needed to facilitate detachment of atoms from supported NCs to reach the gallery.

Submitted for JCP Special Collection in Honor of Women in Chemical Physics and Physical Chemistry

I. INTRODUCTION

Recent studies by Thiel and coworkers[1-6] have demonstrated that deposition of various metals on sputtered graphite can lead to the formation of intercalated or encapsulated metal nanoclusters (NCs) in the gallery between graphene layers just underneath the surface. Under suitable conditions, the point defects formed by sputtering can act as portals for deposited atoms to reach the subsurface gallery. Intercalated few-layer NCs were formed for Dy,[1] Ru,[2] and Pt,[3] and larger three-dimensional (3D) NCs were formed for Cu[4,5] and Fe.[6,7] Ag and Au did not intercalate.[3] An earlier study by Büttner *et al*.[8] indicated intercalation of small Cs clusters adjacent to portals. This phenomenon offers opportunity to synthesize a novel new class of surface nanostructures with multiple potential applications, e.g., formation of catalytic nanoclusters stable against oxidation or coarsening, and facilitating catalysis in confined environments,[9,10] protection of plasmonic nanostructures,[11] nanoscale electrodes and heat sinks in micro- and nanoelectronics,[12,13] etc. The phenomenon also stands in contrast to traditional deposition studies where supported metal NCs are formed during deposition on top of surfaces such as graphite.[14,15] These NCs generally have a 3D form for metals on such weakly-adhering substrates,[15] and are susceptible to coarsening.[16,17]

Indeed, there is a long history of analysis of supported metal nanostructures, sometimes with non-equilibrium growth shapes, formed by surface deposition often in

well-controlled ultrahigh vacuum environments. As early as the 1960's, supported 3D metal nanoclusters were characterized by TEM and SEM on oxides, sulfides, alkali halides, semiconductors, and carbon supports.[15] AFM has also been used to characterize the above types of systems,[18,19] and STM has been used to image 2D as well as 3D metal NCs on metal, semiconductor, graphite, graphene, etc. surfaces.[14,20,21] Also, from late 1960's, mean-field nucleation theory was developed by Zinsmeister, Venables, and others to describe the nucleation and growth of supported metal NCs during deposition.[22] Nucleation theory for supported NCs subsequently developed into an active topic in non-equilibrium statistical physics with beyond-mean-field analysis and Kinetic Monte Caro (KMC) simulation revealing the failure of mean-field treatments for prediction of more detailed quantities such as the NC size distribution.[20]

In contrast to nucleation theory for supported NCs, there has been little development of appropriate theory for intercalated NCs. One study considered the nucleation of intercalated islands near a single isolated point defect portal with a prescribed flux of atoms injected through the portal into the gallery.[23] The focus was on assessing the nucleation location relative to the portal, as well as the lateral growth shape of intercalated NCs. However, such analysis does not address the non-trivial competition between formation of supported NCs on top of the surface and intercalated NCs, and the feature that the latter are observed to dominate only at sufficiently high temperature. The focus of the current contribution is on development of an appropriate stochastic model for this competitive nucleation process.

This effort is partly guided by observations for the Cu/graphite system[4] where there appears no thermodynamic driving force for the formation of intercalated Cu NCs relative to supported Cu NCs. However, there is a significant energetic preference for individual Cu atoms to be in the gallery versus on the top surface. Thus, formation of intercalated NCs should be regarded as driven by kinetics rather than thermodynamics. We note that an even stronger preference for individual atoms to be in the gallery applies for Ru[2] and Fe,[6] which also have a relatively low thermodynamic preference for intercalated NCs. With regard to the temperature dependence of the deposition process, the key trends for the Cu/graphite system are as follows:[4] (i) the population of intercalated NCs is negligible relative to supported NCs at and below 500 K; (ii) the onset temperature for significant intercalation is between 500 K and 600 K, with substantial populations of both intercalated and supported NCs at 600 K; (iii) the population of intercalated NCs is still substantial, but that of supported NCs is negligible at 800 K. Capturing these general trends is a primary goal of our modeling.

In Sec. II, we provide more information on the system of interest, and describe in detail our stochastic model for the deposition process. Some discussion of basic model behavior is provided in Sec. III, as well as results from KMC simulation for key features of this behavior. Conclusions are provided in Sec. IV.

II. SYSTEM DETAILS AND MODEL FORMULATION

There has been extensive analysis of the defects created by sputtering on graphite or graphene surfaces including characterization of the distribution of sizes and structures.[24,25] A key feature of metal deposition on sputtered graphite is that generally the majority of point defects created on the surface do not act as portals for access to

the underlying gallery, presumably because they are below some critical size.[8] However, many or most defects do act as sites for heterogeneous nucleation of supported NCs.[1-7,14] Furthermore, it is plausible that the first metal atoms to reach these defects may be effectively irreversibly bound (due to strong interaction with undercoordinated carbon atoms), but subsequent atoms are more weakly reversibly bound (reflecting metal-metal interactions).[26] Specifically, it has been shown that saturating less stable step edge configurations on graphene with metal atoms facilitates detachment of subsequently aggregating Cu from the step edge.[26] In any case, our modeling will just track the number of reversibly bound metal atoms at these defects.

A schematic indicating the key ingredients of the deposition process is shown in **Figure 1a**. The system which we model consists of a region of the surface with multiple non-portal surface defects (X) which act as heterogenous nucleation centers for supported NCs, together with a single portal defect. Periodic boundary conditions (PBC) are employed. Surface adsorption sites are represented by a periodic grid as are those in the gallery which is accessed through the portal defect. Below, we describe in detail the various ingredients of our model including our prescription of the associated energetics which is illustrated in **Figure 1b**.

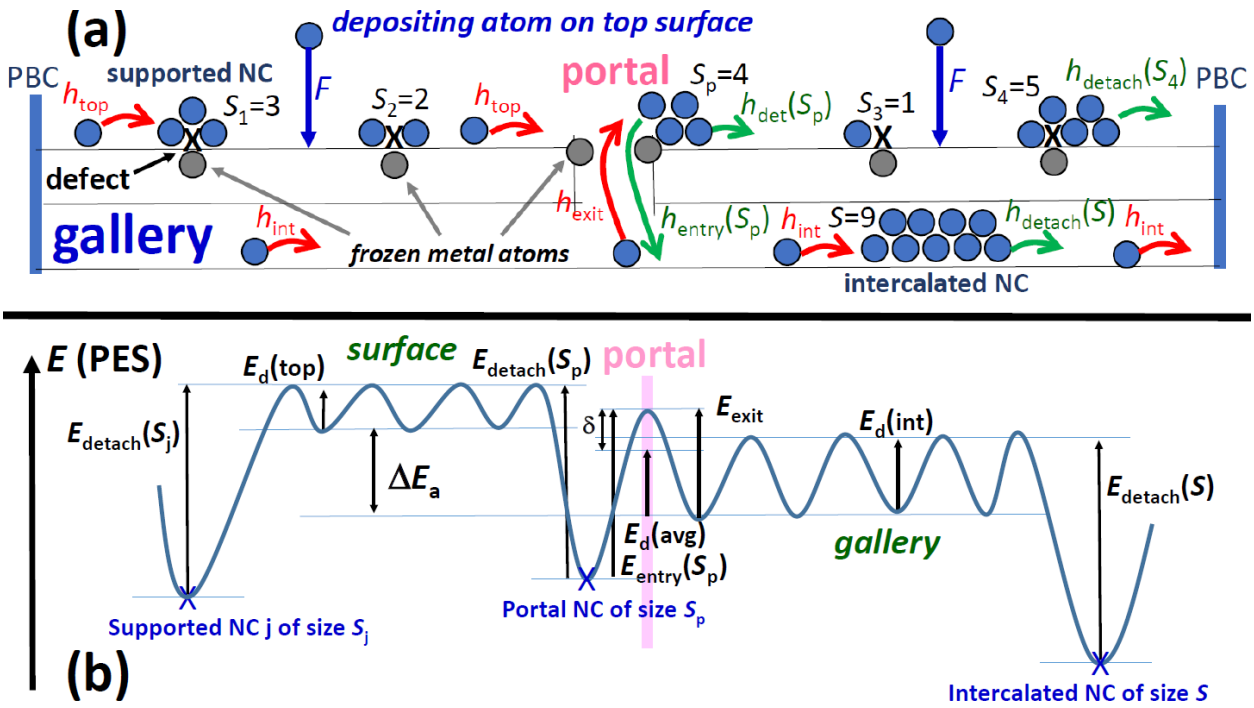

Figure 1. **(a)** Schematic illustrating various processes controlling competitive nucleation and growth of supported NCs versus NCs intercalated in the gallery beneath the surface of a layered material such as graphite. S_j (S_p) denotes the number of reversibly bound atoms (blue) in the NC at defect j (at the portal). This does not include effectively irreversibly bound atoms (grey). S denotes the number of atoms in the one intercalated NC shown (but multiple intercalated NCs can form). **(b)** Potential Energy Surface (PES) or landscape corresponding to the intercalation process showing the PES experienced by an atom on the surface and in the gallery and in transition between them in the presence of supported and intercalated NCs.

Deposition, diffusion, aggregation, and intercalation. In the model, atoms are deposited on the top surface at a prescribed rate, F. Atoms then undergo diffusive hopping between adjacent adsorption sites across the surface and in the gallery. For these and all other thermally-activated hopping processes, hop rates have an Arrhenius form $h = \nu \exp(-\beta E_{act})$, where E_{act} is the corresponding activation barrier, ν is the attempt frequency, and $\beta = 1/(k_B T)$ is the inverse temperature (for temperature T and Boltzmann constant k_B). Deposited atoms hop between adjacent adsorption sites at rate h_{top} with barrier $E_d(\text{top})$ for adatoms on the top surface, and at rate h_{int} with barrier $E_d(\text{int})$ for intercalated atoms the gallery. Atoms reaching defects or the portal can reversibly aggregate with atoms accumulated into NCs at those sites. Detachment leads to further diffusion across the surface, but for the portal, detachment can also lead to reversible entry into the gallery. (Although not implemented here, one could also choose that entry to the gallery is blocked if the size S_p of the NC at the portal is above a threshold value.) No homogeneous nucleation of new NCs is allowed on the top surface since the density of defects is sufficiently high to suppress this process. In contrast, only homogeneous nucleation is active in the gallery which is regarded as defect free.

An important aspect of surface thermodynamics is the need to specify distinct adsorption energies, $E_a(\text{top}) < 0$ and $E_a(\text{int}) < 0$, for an isolated adatom on the top surface and intercalated in the gallery, respectively. A key model parameter is

$$\Delta E_a = E_a(\text{top}) - E_a(\text{int}), \tag{1}$$

where $\Delta E_a > 0$ if intercalation of individual atoms is energetically preferred.

NC energetics and attachment-detachment kinetics. A complete prescription of the deposition process also requires specification of attachment-detachment rates associated with NCs, where the latter generally depend on NC size and reflect system thermodynamics. To this end, we must specify the energy, $E_S(\text{top}) < 0$, associated with a supported NC composed of S reversibly attached atoms. We adopt the form

$$E_S(\text{top}) = -E_c\, S + C_{top}\, S^{2/3} + A_{top}, \tag{2}$$

where $E_c > 0$ denotes the bulk cohesive energy for the metal, and the second term accounts for the contribution from surface and interface energies. The value of A_{top} is not relevant as model behavior depends only on differences in these energies. Within a continuum treatment for large NC sizes, an explicit form for C_{top} can be obtained in terms of these energies for simple models of NC geometry. However, instead we will choose C_{top} to reasonably capture behavior for small NC sizes. For simplicity, in our simulation study, we will not discriminate between the energetics of NCs at defects and at the portal. Of particular importance is the energy change,

$$\Delta E_s(\text{top}) = E_a(\text{top}) + E_{S-1} - E_S = E_a(\text{top}) + E_c - C_{top}[S^{2/3} - (S-1)^{2/3}], \tag{3}$$

upon detachment of an atom from a supported NC of size S whereby the atom then resides on the top surface. Note that ΔE_s increases monotonically with S with a limiting value of $E_c + E_a(\text{top})$, as $S \to \infty$. The energy change for $S = 1$, i.e., detachment of the last reversibly bound metal atom from other irreversibly bound metal atoms (to undercoordinated carbon atoms) in the supported NC, $\Delta E_1(\text{top}) = E_a(\text{top}) - E_1 = E_a(\text{top}) + E_c - C_{top}$, should correspond to the strength of 2-3 nearest-neighbor metal-metal

bonds, thus determining C_{top}. For example, for Cu where E_c = 3.5 eV and E_a(top) = -0.5 eV,[4,19] if one selects $\Delta E_1 \approx 1.0$ eV, then $C_{top} \approx 2.0$ eV.

A similar treatment applies for the energy change, ΔE_S(int), upon detachment of an atom from an intercalated NC. However, these NC are nucleated homogeneously and now S = 1 corresponds to an isolated adatom. Thus, we refine (2) to assign

$$E_S(\text{int}) = -E_c(S-S^*) + C_{int}(S-S^*)^{2/3} + A_{int}, \text{ for } S \geq S^*, \quad (4)$$

and E_S(int) = A_{int}, for $S \leq S^*$. Here, S^* can be regarded as a critical size such that there are negligible interactions within NCs for $S \leq S^*$. The energy change, ΔE_S(int), upon detachment of an atom from an intercalated NC of size S to the gallery follows immediately from (4) where again this quantity increases monotonically with increasing S with a limiting value of $E_c + E_a$(int), as $S \to \infty$. The energy change ΔE_{S^*+1}(int) = E_a(int) + E_c - C_{int}, should also correspond to the strength of 2-3 nearest-neighbor metal-metal bonds, thus determining C_{int} (so $C_{int} \approx 1.5$ eV for Cu with E_a(int) = -1.0 eV[4,21]). We will select S^* = 1 in our simulations.

Assuming that there is no additional barrier for attachment of atoms to NCs, i.e., that $h_{attach} = h_{top}$ ($h_{attach} = h_{int}$) for the rate of attachment to NCs on the top surface (in the gallery), it follows from detailed-balance that the detachment rate for supported (top) and intercalated (int) NCs of S atoms satisfies

$$h_{detach}(\text{top}) = h_{top} \exp[-\beta \Delta E_s(\text{top})] \text{ and } h_{detach}(\text{int}) = h_{int} \exp[-\beta \Delta E_s(\text{int})]. \quad (5)$$

Intercalation kinetics. Next, we describe the kinetics of intercalation, i.e., the assignment of entry and exit rates to and from the gallery for atoms at the portal defect. One regards the entry of atoms to the gallery as associated with detachment from an NC at the portal, rather than a direct transition from the surface to the gallery. This is reasonable since the first atoms to reach the portal will likely be strongly bound at its edge, and atoms subsequently entering the gallery will have to overcome their bonding to such metal atoms. In fact, reversibly attached metal atoms can either detach to the top surface or to the gallery. The rate of exit from the gallery, i.e., the rate for an intercalated atom just below the portal (which is not incorporated in an NC) to attach to the NC at the portal is selected to be $h_{exit} = h_{avg} \exp(-\beta\delta)$, where $h_{avg} = (h_{top}\, h_{int})^{1/2} = \nu \exp[-\beta E_d(\text{avg})]$, with $E_d(\text{avg}) = \frac{1}{2}[E_d(\text{top}) + E_d(\text{int})]$, and δ corresponds to a possible additional Ehrlich-Schwoebel type barrier to pass through the portal. In the absence of such a barrier, the exit rate is chosen as a geometric average of hop rates on the surface and in the gallery, although the specifics of such a choice will not significantly impact model behavior.

For an atom in the NC at the portal, it can either detach to the top surface with rate $h_{detach} = h_{top} \exp[-\beta \Delta E_s(\text{top})]$ as noted above, or it can enter the gallery with rate

$$h_{entry} = h_{exit} \exp[-\beta \Delta E_s(\text{int})] = h_{exit} \exp[-\beta \Delta E_s(\text{top})] \exp[\beta \Delta E_a]. \quad (6)$$

The form (6) accounts for detailed-balance noting that entry to the gallery is the reverse process of exiting the gallery. In the case where $h_{top} = h_{int}$ (a reasonable choice which we will adopt in simulations), and if $\delta = 0$ (a choice which effectively captures experimental observations), then it follows from (6) that

$h_{entry}/h_{detach} = \exp(\beta \Delta E_a)$. (7)

Again, one has that $\Delta E_a > 0$ for stronger adsorption in the gallery than on the top surface. Thus, (7) indicates that portal entry is naturally enhanced relative to detachment to the top surface by stronger adsorption of atoms in the gallery.

Point Island Modeling (PIM). Our focus is on determining the relative rates of formation of supported versus intercalated NCs, and also the sizes of those NCs, rather than the details of NC structure. Given the complexity of the deposition process, we adopt a "point island modeling" (PIM) strategy which suppresses NC structure by regarding NCs as occupying a single site on the relevant adsorption site lattice. However, the PIM attaches a label to each NC to track its size, so attachment and detachment processes lead to a change in this size label by +1 and -1, respectively.[27] The PIM strategy has proven particularly useful for efficient code development and simulation of a variety of complex NC nucleation and growth processes.[20,28,29] A schematic of our PIM implementation of the deposition process is provided in **Figure 2**. We will also adopt the format of **Figure 2** (i.e., showing side-by-side the state of the top surface and the gallery) when presenting results of KMC simulations in Sec. III. We choose a square grid to represent adsorption sites on the surface and in the gallery, but the choice of grid geometry does not significantly impact the basic features of the diffusion-mediated process of interest. Also, a designated number of surface adsorption sites on the grid are assigned as defect sites which facilitate heterogeneous nucleation of supported NCs, and a single site is designated as the portal (located in the center of the schematic grid and in the center of our simulation images below).

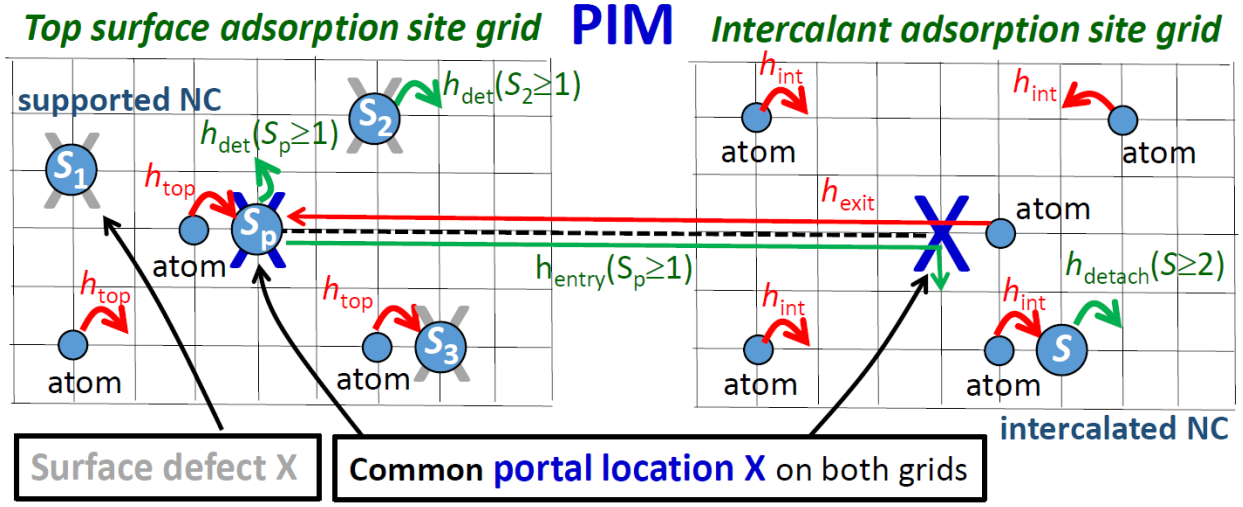

Figure 2. Schematic of the Point Island Model (PIM). Two adsorption site grids for the top surface and gallery are coupled through the portal defect site where the intercalation of atoms occurs. NCs are represented as a single occupied site, as are isolated atoms, but NCs carry a size label (S, S_j, S_p) as indicated.

III. MODEL BEHAVIOR AND KMC SIMULATION RESULTS

With regard to model behavior, it might be anticipated that for lower temperatures: (i) deposited atoms will readily aggregate into NCs at surface defects and at the portal leading to heterogeneous nucleation of numerous supported NCs; (ii) detachment from these NCs will be sufficiently inhibited that their growth will incorporate effectively all deposited atoms, so that a negligible number of deposited atoms will detach from the NC at the portal to reach the gallery. For significant intercalation, at least detachment from the smallest NCs must be facile on the time scale of aggregation. This will allow detached atoms to reach the gallery where they are more strongly adsorbed, and avoid growth of supported NCs to the point where detachment is effectively inoperative (noting that detachment rate decrease with increasing NC size since ΔE_s(top) increases with S). We validate this picture for our model below.

To perform KMC simulations, we must first assign all model parameters. One complication is that metals such as Cu have very low diffusion barriers on the top graphite surface and in the gallery. This leads to extremely high values of hop rates relative to the deposition rate, e.g., $h_{top}/F \sim 10^{14}$ s^{-1} at 600 K or higher for typical F = 0.05 monolayers (ML)/s. Such high values make simulation computationally prohibitive at least for reversible NC formation. Thus, we scale down rates h_{top} and h_{int} in our simulations. However, since detachment rates are proportional to these reduced rates, we also scale down metal interaction energies relative to values for Cu so as to maintain detachment rates at reasonable values. Our default parameter choice sets F = 0.05 ML/s, $h_{top} = h_{int} = 10^7$ s^{-1} at 600 K, so that $h_{top}/F = h_{int}/F = 2 \times 10^8$, E_a(top) = -0.35 eV with E_a(int) given below, E_c = 2.55 eV, C_{top} = 1.78 eV, C_{int} = 1.17 eV, δ = 0 unless stated otherwise, and S^* = 1. For system size, we choose a square $L \times L$ grid of adsorption sites for the top surface and the gallery with PBC and L = 141 corresponding roughly to a 30 × 30 nm^2 region of graphite. We include 40 non-portal defects and 1 portal defect in this region. The amount of metal deposited is always 0.1 ML.

First, we explore the dependence of behavior on $\Delta E_a = E_a$(top) - E_a(int) ≥ 0 as we have argued that this is a key parameter driving intercalation. **Figure 3** shows KMC simulation results for the distribution of supported and intercalated NCs at 600 K for ΔE_a = 0.30, 0.25, and 0.00 eV. Results for additional values of ΔE_a are shown in the Supplementary Materials (SM). For ΔE_a = 0.30 eV, the driving force for intercalation is sufficiently strong that intercalated NCs start to dominate supported NCs (and below we show similar behavior for ΔE_a = 0.35 eV). On the other hand, reducing ΔE_a to 0.25 eV, supported NCs start to dominate, and for ΔE_a = 0 there is little formation of intercalated NCs. This trend is natural as ΔE_a gives the magnitude of the energetic preference for isolated atoms to be in the gallery versus on the top surface. The corresponding enhancement in the density of such intercalated atoms facilitates the nucleation of intercalated NCs. Again, we regard this enhancement as a kinetic phenomenon as there is no thermodynamic preference for intercalated versus supported NCs in our model (or in systems like Cu/graphite).

Second, we assess the effect of temperature on intercalation. Here, we set E_a(int) = -0.70 eV, so that ΔE_a = 0.35 eV. Temperature dependence is appropriately incorporated into detachment rates given their Arrhenius form. However, $h_{top}/F = h_{int}/F$ also are impacted by and increase with temperature. Thus, for simulations at 800 K, we

increase these values to 2×10^9 (recalling that $h_{top}/F = h_{int}/F = 2 \times 10^8$ at 600 K), and for simulations at 500 K, they are decreased to 3.2×10^7. This variation corresponds to an Arrhenius form for hop rates, but again not with physical diffusion barriers which produce much higher ratio values. **Figure 4** shows KMC simulation results for the distribution of supported and intercalated NCs at 500, 600, and 800 K. Behavior is quite consistent with the trends described in Sec. I for the Cu/graphite system. Supported NCs dominate at 500 K with a crossover to a slight preference for intercalated NCs at 600 K, and an overwhelming dominance of intercalated NCs at 800 K. Further elucidation of this behavior follows based on comparative analysis of relevant aggregation and detachment rates.

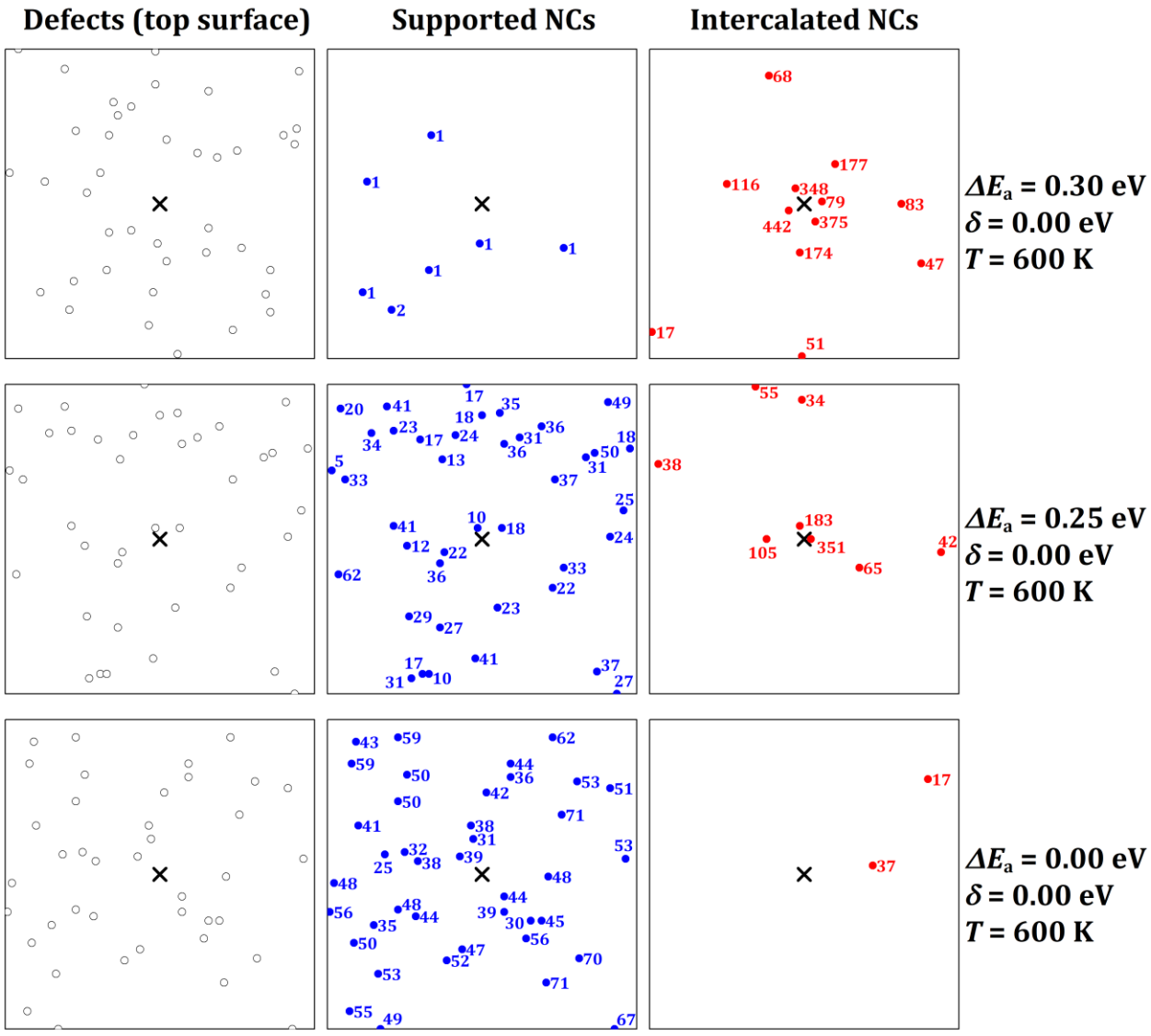

Figure 3. KMC simulation results for the dependence of intercalation behavior on $\Delta E_a = E_a(\text{top}) - E_a(\text{int}) \geq 0$ (the energetic preference for atoms to be in the gallery versus on the top surface). Left: distribution of surface defects where × denotes the portal location. Middle: distribution of supported NCs. Right: distribution of intercalated NCs. NC size in atoms is also indicated.

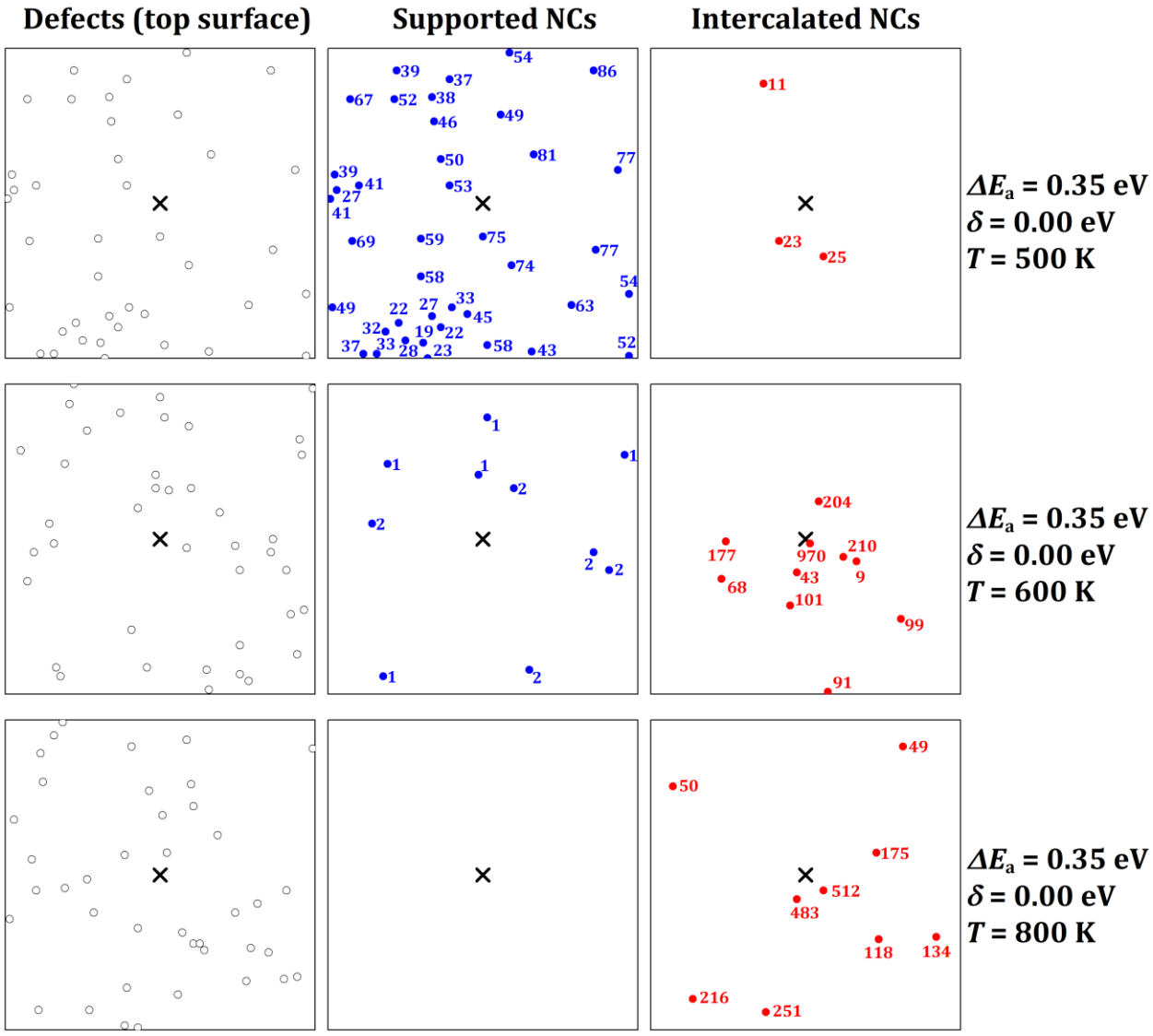

Figure 4. KMC simulation results for the dependence on temperature of intercalation behavior. Left: distribution of surface defects where × denotes the portal location. Middle: distribution of supported NCs. Right: distribution of intercalated NCs. NC size in atoms is also indicated.

The behavior observed in **Figure 4** can be more fully understood comparing the mean rate of aggregation, R_{agg}, of deposited atoms with NCs at each surface defect with the rate of detachment from those NCs. The capture zone area for each defect (corresponding to the reciprocal of the defect density) equals A_{CZ} = 485 adsorption sites, so that $R_{agg} = F\,A_{cz}$ = 0.041 s^{-1}. The rate of detachment of atoms from supported NCs equals h_{detach}(top) = $10^{1.9}$ ($10^{-5.4}$) for S = 1 (2) at 500 K. The lifetime $\tau_1 = 1/h_{detach}$(top) = 0.013 s for single (S = 1) atoms at defects at 500 K is a significant fraction of the time $\tau_{agg} = 1/R_{agg}$ = 0.041 s between aggregation events. Thus, such atoms will generally be incorporated into NCs of size $S \geq 2$ from which detachment is

effectively inoperative, thereby inhibiting atoms from reaching the portal. In contrast, one has that $h_{detach}(top) = 10^{3.5}$ ($10^{5.4}$) s^{-1}, for $S = 1$ at 600 K (800 K), so that now the lifetime for single ($S = 1$) atoms at defects is negligible compared to τ_{agg} and such atoms can readily detach and reach the portal to intercalate.

The model incorporates many parameters, and simulation can be utilized to effectively assess the dependence of model behavior on any of these. Our analysis above focused on the dependence on ΔE_a and on temperature while not incorporating any additional barrier for entry and exit to the gallery (i.e., selecting $\delta = 0$). Naturally, formation of intercalated NCs should be inhibited for sufficiently high values of δ. Indeed, retaining other model parameters as in **Figure 4**, we find that the population of intercalated NCs at 600 K is somewhat suppressed for $\delta = 0.3$ eV, and significantly reduced for $\delta = 0.4$ eV. See the SM.

IV. CONCLUSIONS

Analysis of competitive nucleation and growth of intercalated versus supported NCs during deposition of various metals on sputtered graphite, and specifically of the dominant formation of intercalated NCs at higher temperature, has been advanced in the last few years by Thiel and coworkers.[1-7] This competitive process is naturally more complex process than traditional nucleation and growth of just supported NCs. Nonetheless, suitable stochastic modeling appropriately accounting for key surface energetics and kinetics, and utilizing a PIM strategy to simply model development and simulation while retaining key features of the process, is able to elucidate basic trends observed in experiments.

As noted in Sec. I, not all metals intercalate into sputtered graphite. Recent analysis indicates a strong correlation between the Shannon effective ionic radius and preference for individual metal atom to intercalate versus adsorb on the top surface. At least for elements with ionic-like bonding, atoms with smaller radii have a stronger preference to intercalate.[30] Our analysis is targeted to describe the type of behavior seen for elements with smaller ionic radii such as Cu[4], and to some extent also by Ru[2] and Fe[6]. In these systems, there is a significant preference for isolated metal atoms to reside in the gallery versus on the top surface, but there is no significant thermodynamic driving force for the formation of intercalated versus supported NCs. Thus, system kinetics is a key determinant of behavior.

We find that essential features driving the experimentally observed transition from dominance of supported to intercalated NCs with increasing temperature are: the facile detachment of atoms from supported NCs at higher temperature, and the significant energetic preference for isolated atoms to reside in the gallery. Facile detachment of atoms from smaller supported NCs avoids NC growth to sizes where detachment is strongly inhibited which would lead to most deposited atoms becoming effectively irreversibly incorporated into these surface NCs. Detaching atoms can reach the portal and access the energetically preferred gallery where their higher density facilitates homogeneous nucleation of intercalated NCs.

SUPPLEMENTARY MATERIAL

See the Supplementary Material providing additional results for the dependence of model behavior on: (S1) the energetic preference, ΔE_a, for metal atoms to be in the gallery; and (S2) an additional barrier, δ, for entry and exit to the gallery.

DEDICATION

This paper is dedicated to Patricia A. Thiel who performed groundbreaking work on the formation and stability of metal nanostructures on surfaces, and recently on metal nanostructures intercalated under surface of layered materials (the topic of this contribution). She is also broadly recognized for her studies on chemisorption of water and of chalcogens on metal surfaces, and for pioneering analyses of quasicrystal surface structure.

ACKNOWLEDGEMENTS

YH and JWE performed the theoretical model development and simulation reported in this study, and were supported by the US Department of Energy, Office of Science, Basic Energy Sciences, Division of Chemical Sciences, Geosciences, and Biosciences through the Ames Laboratory Chemical Physics project. ALR and MCT provided experimental insights and were supported by the US Department of Energy, Office of Science, Basic Energy Sciences, Division of Materials Sciences and Engineering. This work was performed at Ames Laboratory which is operated by Iowa State University under contract No. DE-AC02-07CH11338.

DATA AVAILABILITY

The data that support the findings of this study are available within the article and its supplementary material and from the corresponding author upon reasonable request.

REFERENCES

1. Y. Zhou, A. Lii-Rosales, M. Kim, M. Wallingford, D. Jing, M. C. Tringides, C.-Z. Wang, and P. A. Thiel, Carbon 127, 305 (2018).

2. A. Lii-Rosales, Y. Han, K. M. Yu, D. P. Jing, N. Anderson, D. Vaknin, M. C. Tringides, J. W. Evans, M. S. Altman, and P. A. Thiel, Nanotechnology 29, 505601 (2018).

3. A. Lii-Rosales, Y. Han, D. P. Jing, M. C. Tringides, and P. A. Thiel, Phys. Rev. Res. 2, 033175 (2020).

4. A. Lii-Rosales, Y. Han, J. W. Evans, D. Jing, Y. Zhou, M. C. Tringides, M. Kim, C. Z. Wang, and P. A. Thiel, J. Phys. Chem. C 122, 4454 (2018).

5. S. E. Julien, A. Lii-Rosales, K.-T. Wan, Y. Han, M. C. Tringides, J. W. Evans, and P. A. Thiel, Nanoscale 11, 6445 (2019).

6. A. Lii-Rosales, Y. Han, K. C. Lai, D. Jing, M. C. Tringides, J. W. Evans, and P. A. Thiel, J. Vac. Sci. Technol. A 37, 061403 (2019).

7. A. Lii-Rosales, Y. Han, S. E. Julien, O. Pierre-Louis, D. Jing, K.-T. Wan, M. C. Tringides, J. W. Evans, and P. A. Thiel, New J. Phys. 22, 023016 (2020).

8. M. Büttner, P. Choudhury, J.K. Johnson, and J. T. Yates Jr., Carbon 49, 3937 (2011).

9. T. Yang, Y. Huang, L. Yang, X. Li, X. Wang, G. Zhang, Y. Luo, and J. Jiang, J. Phys. Chem. Lett. 10, 3129 (2019).

10. Q. Fu and X. Bao Surface chemistry and catalysis confined under two-dimensional materials Chem. Soc. Rev. 46, 1842 (2017).

11. V. G. Kravets, R. Jalil, Y.-J. Kim, D. Ansell, D. E. Aznakayeva, B. Thackray, L. Britnell, B. D. Belle, F. Withers, I. P. Radko, Z. Han, S. I. Bozhevolnyi, K. S. Novoselov, A. K. Geim, and A. N. Grigorenko, Scientific Reports 4, 5517 (2014).

12. G. Fiori, F. Bonaccorso, G. Iannaccone, T. Palacios, D. Neumaier, A. Seabaugh, S. K. Banerjee and L. Colombo, Nat. Nanotechnol. 9, 768 (2014).

13. A. Allain, J. Kang, K. Banerjee, and A. Kis, Nat. Mater. 14, 1195 (2015).

14. D. Appy, H. Lei, C.-Z. Wang, M. C. Tringides, D.-J. Liu, J. W. Evans, and P. A. Thiel, Prog. Surf. Sci. 89, 219 (2014).

15. R. Kern, G. Le Lay, and J.J. Metois, in Current Topics in Materials Sciences Vol. 3, edited by E. Kaldis (North Holland, Amsterdam, 1979) Ch.3

16. M. Zinke-Allmang, L.C. Feldman, and M.H. Grabow, Surf. Sci. Rep. 16, 377 (1992).

17. K.C. Lai, Y. Han, P. Spurgeon, W. Huang, P.A. Thiel, D.-J. Liu, and J.W. Evans, Chem. Rev. 119, 6670 (2019).

18. E. Dokou, W.E. Farneth, and M.A. Barteau, Studies in Surface Science and Catalysis 130, 3167 (2000).

19. D. Jing, A. Lii-Rosales, K.C. Lai, Q. Li, J. Kim, M.C. Tringides, J.W. Evans, and P.A. Thiel, New J. Phys. 22, 053033 (2020).

20. J. W. Evans, P. A. Thiel, and M. C. Bartelt, Surf. Sci. Rep. 61, 1 (2006).

21. X. Liu, Y. Han, J. W. Evans, A. K. Engstfeld, R. J. Behm, M. C. Tringides, M. Hupalo, H.-Q. Lin, L. Huang, K.-M. Ho, D. Appy, P. A. Thiel and C.-Z. Wang, Prog. Surf. Sci. 90, 397 (2015).

22. J. A. Venables, Phil. Mag. 27, 697 (1973).

23. Y. Han, A. Lii-Rosales, Y. Zhou, C. J. Wang, M. Kim, M. C. Tringides, C. Z. Wang, P. A. Thiel, and J. W. Evans, Phys. Rev. Materials 1, 053403 (2017).

24. M. Nastasi, J. Mayer, and J. Hirvonen, *Ion-solid interactions - fundamentals and applications* (Cambridge University Press, Cambridge 1996).

25. O. Lehtinen, J. Kotakoski, A. V. Krasheninnikov, A. Tolvanen, K. Nordlund, and J. Keinonen, Phys. Rev. B 81, 153401 (2010).

26. Y. Han, A. Lii-Rosales, M.C. Tringides, J.W. Evans, and P.A. Thiel, Phys. Rev. B 99, 115415 (2019).

27. M.C. Bartelt and J. W. Evans, Phys. Rev. B 46, 12675 (1992).

28. J.A. Meyer and R.J. Behm, Surf. Sci. Lett. 322, L275 (1996).

29. Y. Han, E. Gaudry, T. J. Oliveira, and J. W. Evans, J. Chem. Phys. 145, 21004 (2016).

30. W. Li, L. Huang, M.C. Tringides, J.W. Evans, and Y. Han, J. Chem. Phys. Lett., in press (2020). https://dx.doi.org/10.1021/acs.jpclett.0c02887